

Distinct Innate Immune Phagocyte Responses to *Aspergillus fumigatus* Conidia and Hyphae in Zebrafish Larvae

Benjamin P. Knox,^{a,b} Qing Deng,^{b*} Mary Rood,^c Jens C. Eickhoff,^d Nancy P. Keller,^{b,e} Anna Huttenlocher^{b,f}

Microbiology Doctoral Training Program, University of Wisconsin—Madison, Madison, Wisconsin, USA^a; Department of Medical Microbiology and Immunology, University of Wisconsin—Madison, Madison, Wisconsin, USA^b; Laboratory of Genetics, University of Wisconsin—Madison, Madison, Wisconsin, USA^c; Department of Biostatistics and Medical Informatics, University of Wisconsin—Madison, Madison, Wisconsin, USA^d; Department of Bacteriology, University of Wisconsin—Madison, Madison, Wisconsin, USA^e; Department of Pediatrics, University of Wisconsin—Madison, Madison, Wisconsin, USA^f

***Aspergillus fumigatus* is the most common filamentous fungal pathogen of immunocompromised hosts, resulting in invasive aspergillosis (IA) and high mortality rates. Innate immunity is known to be the predominant host defense against *A. fumigatus*; however, innate phagocyte responses to *A. fumigatus* in an intact host and their contributions to host survival remain unclear. Here, we describe a larval zebrafish *A. fumigatus* infection model amenable to real-time imaging of host-fungal interactions in live animals. Following infection with *A. fumigatus*, innate phagocyte populations exhibit clear preferences for different fungal morphologies: macrophages rapidly phagocytose conidia and form aggregates around hyphae, while the neutrophil response is dependent upon the presence of hyphae. Depletion of macrophages rendered host larvae susceptible to invasive disease. Moreover, a zebrafish model of human leukocyte adhesion deficiency with impaired neutrophil function also resulted in invasive disease and impaired host survival. In contrast, macrophage-deficient but not neutrophil-deficient larvae exhibited attenuated disease following challenge with a less virulent (Δ *laeA*) strain of *A. fumigatus*, which has defects in secondary metabolite production. Taking these results together, we have established a new vertebrate model for studying innate immune responses to *A. fumigatus* that reveals distinct roles for neutrophils and macrophages in mediating host defense against IA.**

Aspergillus fumigatus is an airborne opportunistic human pathogen. Infectious particles for *A. fumigatus* are airborne asexual spores called conidia. As a consequence of their small size (2 to 3 μ m) and worldwide distribution, inhaled conidia readily enter the deep recesses of the lung, and it is estimated that the average individual inhales up to several hundred conidia per day (1). In an immunocompetent host, inhaled conidia are efficiently contained, generally with no pathological consequences. In contrast, immunocompromised populations are at risk for developing invasive aspergillosis (IA), a devastating disease characterized by conidial germination into tissue-penetrating hyphae growing beyond the original site of infection. While defects in adaptive immunity can predispose individuals to IA (2, 3), the majority of cases result from impaired innate immune function. Increased uses of immunosuppressive therapies for advanced medical treatments over the last several decades have been accompanied by an increase in the number of patients developing IA (4, 5). Despite advances in early diagnosis and treatment, mortality rates from IA can be as high as 90% in the most at-risk populations (1, 6, 7). Furthermore, disease pathology can vary significantly depending on the immunosuppressant used and immune status of the host (8, 9), suggesting a dynamic interplay between elements of the innate immune system and *A. fumigatus*.

Mammalian models, most often murine, currently use several methods for immune suppression to induce IA. For example, administration of cytotoxic compounds and corticosteroids such as cyclophosphamide and cortisone acetate is used to cause neutropenia and overall immune suppression. While broad immunosuppression is effective in recapitulating many facets of IA (e.g., tissue lesions, dissemination, and mortality), it becomes difficult to draw conclusions about the contribution of specific phagocyte populations to host survival (10, 11). More specific immune suppression in mouse models has been attained with monoclonal

antibody-mediated neutrophil depletion and clodronate liposome-mediated macrophage depletion (12). Again, innate immune contributions to controlling IA can be masked even with targeted approaches, as nontargeted innate and adaptive functions that contribute to host recognition of *A. fumigatus* (13) can remain functional.

The larval zebrafish (*Danio rerio*) is an increasingly popular model system to study innate defenses against pathogens in a vertebrate host because adaptive immunity does not develop until several weeks after fertilization (14). The larval zebrafish innate immune system exhibits a high degree of functional competence and conservation with mammals. Within days after fertilization, larvae have both macrophage and neutrophil populations equipped with conserved pathogen recognition receptors, oxidative mechanisms, and phagocytic behaviors (15) as well as dynamic innate transcriptional profiles in response to pathogens (15, 16). While well established as an infection host for bacterial pathogens (17), the larval zebrafish has not frequently been used to model fungal disease. However, recent studies have highlighted the role of innate immunity in response to the fungal pathogen

Received 29 March 2014 Accepted 19 May 2014

Published ahead of print 30 May 2014

Address correspondence to Nancy P. Keller, npkeller@wisc.edu, or Anna Huttenlocher, huttenlocher@wisc.edu.

* Present address: Qing Deng, Department of Biological Sciences, Purdue University, West Lafayette, Indiana, USA.

Supplemental material for this article may be found at <http://dx.doi.org/10.1128/EC.00080-14>.

Copyright © 2014, American Society for Microbiology. All Rights Reserved.
doi:10.1128/EC.00080-14

Candida albicans using zebrafish (18–20). Furthering its utility as an infection host, the larval zebrafish is amenable to rapid genetic manipulation through morpholino-mediated (MO) gene knock-down (21), straightforward genomic editing (22), and forward genetic approaches (23). The availability of transgenic lines harboring fluorescently labeled phagocytes coupled with inherent optical transparency at the larval stage enables noninvasive *in vivo* imaging of immune function at the cellular level (24). Finally, their small size and facile husbandry make the larval zebrafish ideal for high-throughput analysis where large larval numbers give strong statistical power to survival analysis and studies of phagocyte behavior.

We sought to exploit the advantages of the larval zebrafish to expand host-*Aspergillus* interaction studies to a genetically tractable, optically transparent host that is dependent upon innate immunity and amenable to high-throughput survival analysis. We uncovered several advantages of this model over the murine model of IA, chief of which is the ability to noninvasively visualize real-time phagocyte interactions with both spore and hyphal morphologies of *A. fumigatus* in an intact host. The power of real-time imaging has allowed for elucidation of previously uncharacterized roles for both macrophages and neutrophils in mediating distinct elements of host survival against *A. fumigatus*. Furthermore, we used the sensitivity of this model to reveal host immunosuppression-specific virulence attenuation for a Δ laeA strain of *A. fumigatus*. Our larval zebrafish model offers an accessible and high-throughput resource for studying the mechanisms mediating host resistance and susceptibility to, as well as precise virulence determinants for, the increasingly problematic opportunistic pathogen *A. fumigatus*.

MATERIALS AND METHODS

Zebrafish care and maintenance. Adult zebrafish were kept under a light/dark cycle of 14 h and 10 h, respectively. Larval zebrafish were incubated at 28.5°C in E3 buffer. For infection experiments, larvae were switched to E3 made without methylene blue (E3-MB) at 24 h postinfection (hpi) and manually dechorionated between 24 and 30 hpi. Prior to microinjection or imaging, larvae were anesthetized in E3-MB containing 0.2 mg/ml Tricaine (ethyl 3-aminobenzoate; Sigma-Aldrich). For live imaging, pigment synthesis was inhibited by switching larvae to E3-MB containing 0.2 nM 1-phenyl-2-thiourea (PTU) (Sigma-Aldrich) at 24 h postfertilization (hpf). For time lapse imaging, larvae were mounted in 1% low-melting-point agarose, 0.2 mg/ml Tricaine, and 0.2 nM PTU (final concentrations) on a custom-made glass-bottom dish. When necessary, larvae were gently dissected out of the agarose after imaging into E3-MB until being remounted for follow-up imaging. All adult and larval zebrafish procedures were in full compliance with NIH guidelines and approved by the University of Wisconsin—Madison Institutional Animal Care and Use Committee (no. M01570–0–02–13).

Fungal growth conditions and inoculum preparation. Table S1 in the supplemental material lists all fungal strains used in this study. All *A. fumigatus* strains were grown at 37°C on solid glucose minimal medium (sGMM) (25) with supplements as needed. Conidial suspensions for infection experiments were prepared by evenly spreading sGMM with 1×10^6 conidia/plate. After at least 72 h of growth, conidia were harvested with sterile water supplemented with 0.01% Tween and gentle rubbing with an L-style spreader, passed through two layers of sterile Miracloth into a sterile 50-ml screw-cap tube, and brought to a volume of 50 ml. Following centrifugation at $900 \times g$ for 10 min, conidial pellets were thoroughly resuspended in 50 ml sterile phosphate-buffered saline (PBS), pelleted again, and brought to a volume of approximately 5 ml in sterile PBS before passing once more through a double layer of sterile Miracloth. Conidia were then enumerated with a hemocytometer and brought to a

final concentration of 1.5×10^8 conidia/ml in PBS prior to microinjection into zebrafish larvae (see “Conidial microinjection” below). In our hands, this procedure for harvesting, concentrating, and resuspending conidia is ideal for minimizing hyphal fragment contamination and conidial clumping to reduce downstream clogging of the microinjection capillary needle. For heat inactivation, conidia were incubated at 99.0°C for 30 min with gentle agitation. Heat inactivation was verified by plating on GMM for 3 days at 37°C. All prepared conidial suspensions for microinjection were used within 4 weeks.

***Pseudomonas aeruginosa* growth conditions and inoculum preparation.** The *Pseudomonas aeruginosa* strain (PAK) carrying a plasmid-encoded mCherry construct for constitutive expression (pmKB1::mCherry) was kindly provided by S. Moskowitz, University of Washington, Seattle, WA, USA (26). From frozen stock, bacterial colonies were isolated on Luria-Bertani agar supplemented with 200 µg/ml carbenicillin following overnight incubation at 37°C. For injections, approximately 5 to 10 colonies were wiped from the agar surface, suspended in PBS, and adjusted as necessary to a final optical density of 0.1.

Construction of YFP-expressing *A. fumigatus* strain. Table S2 in the supplemental material lists all primers used in this study. Quick-change mutagenesis (27) and double-joint PCR (28) were used to generate transforming DNA for making *A. fumigatus* strain TBK1.1 from the auxotrophic Af293.1 strain (see Table S1 in the supplemental material). Briefly, the yellow fluorescent protein (YFP)-coding sequence was amplified from pSK495 using primers QC-pFNO3-pSK495-F and QC-pFNO3-pSK495-R and used to replace the green fluorescent protein (GFP) sequence of pFNO3 by quick-change mutagenesis. Successful quick-change mutagenesis and generation of pBPK1 were confirmed via restriction mapping and sequencing. Transforming DNA was designed to insert the YFP-pyrG sequence at the 3' end of *A. fumigatus* *gpdA* to create a fusion protein. Double-joint PCR fused, in order, the following fragments to generate a linear transformation construct: AfgpdA5' Flank amplified from *A. fumigatus* genomic DNA with primers AfgpdA-YFP-pyrG-5'F and AfgpdA-YFP-pyrG-5'R, QC-YFP amplified from pBPK1 with primers AfpBPK1-F and AfpBPK1-R, and AfgpdA3' Flank amplified from *A. fumigatus* genomic DNA with primers AfgpdA-YFP-pyrG-3'F and AfgpdA-YFP-pyrG-3'R. The resulting linear DNA construct was transformed into strain Af293.1 (a *pyrG* auxotroph). Fungal protoplasts were generated and transformed as previously described (29). Strain TBK1.1 was selected by reversion to prototrophy and verified by diagnostic PCR using primers AfgpdA-YFP-DIGN-F and AfgpdA-YFP-pyrG-3'R in addition to visual observation of constitutive YFP expression in both spores and hyphae.

MO knockdown. Morpholinos (MOs) were purchased from Gene Tools (Philomath, OR) and stored at room temperature in sterile distilled water at a stock concentration of 1 mM. Three nanoliters of MOs was microinjected into the yolk center of embryos at the 1- to 4-cell developmental stage at the indicated concentrations (pu.1, 500 µM [30]; irf8, 400 µM [31]; Rac2, 100 µM [32]). A standard control MO (Gene Tools) was injected at a concentration matching that of the experimental MO.

Conidial microinjection. In preparation for hindbrain ventricle infection, conidial stocks in PBS at a concentration of 1.5×10^8 conidia/ml were mixed 2:1 with sterile 1% phenol red, for clear visualization of injection success, rendering a final conidial concentration of 1.0×10^8 conidia/ml. After manual dechorionation of embryos at ~28 hpf, localized hindbrain infections were performed with 3-µl infection volumes via the otic vesicle on anesthetized larvae at ~36 hpf as described previously (18) with larvae positioned laterally on injection plates made of 3% agarose in E3 pretreated with 1 ml filter-sterilized 2% bovine serum albumin (BSA) to prevent larval abrasion against the agarose surface and facilitate handling. Under these conditions, individual larvae received on average 50 conidia, and CFU/injection were monitored via injection into 0.1-ml puddles of sterile water on sGMM plates. (See Fig. S1 in the supplemental material for individual larvae homogenizations and CFU enumeration at time zero for the range of initial fungal burdens.) When coinjecting *A. fumigatus*

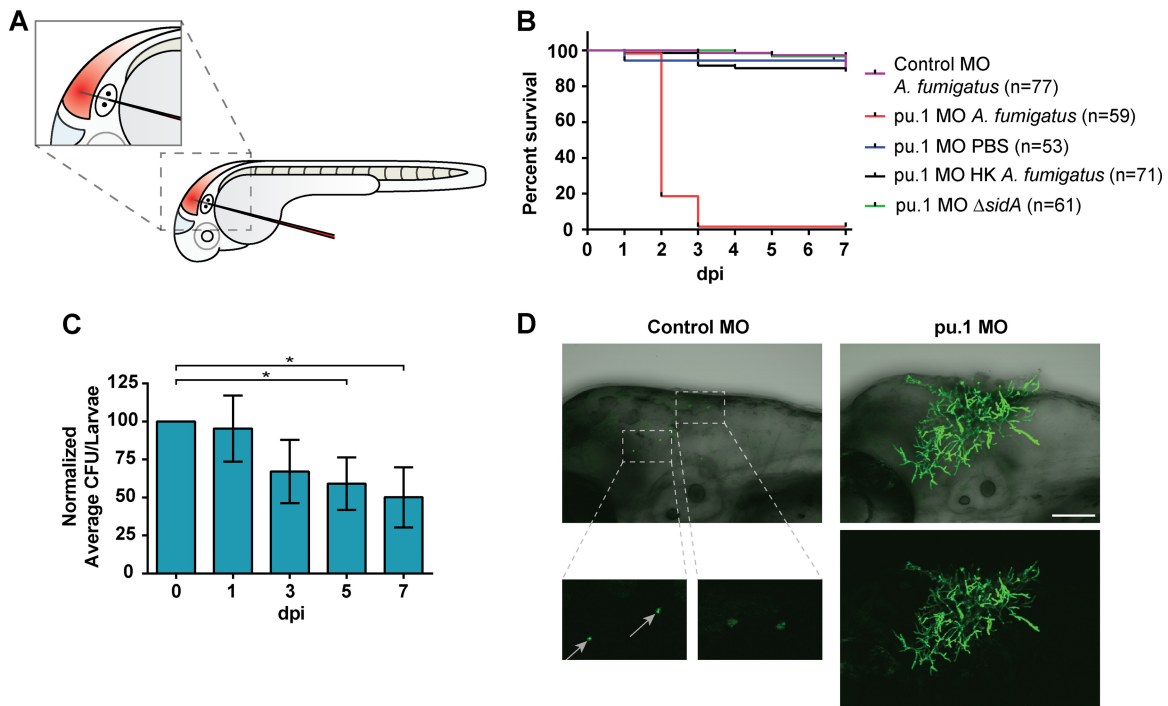


FIG 1 *Aspergillus fumigatus* causes invasive disease in immunodeficient larvae. (A) Cartoon of zebrafish larvae at ~32 hpf undergoing microinjection of conidia into the hindbrain ventricle (shaded red) through the otic vesicle. (B) Immunocompetent larvae (control MO) are not susceptible to infection following challenge with *A. fumigatus* (*gpdA::GFP::his2A*). Treatment with the pu.1 morpholino (pu.1 MO) depletes morphant larvae of macrophages and neutrophils and renders them highly susceptible ($P < 0.0001$) to infection following challenge with *A. fumigatus*. pu.1 morphant larvae showed no mortality following injection of PBS, heat-killed *A. fumigatus* (HK), or the classically avirulent Δ *sidA* strain of *A. fumigatus* deficient in siderophore biosynthesis ($P > 0.05$). Survival data are pooled from three independent experimental replicates, and P values were calculated by Cox proportional-hazard regression analysis. (C) Immunocompetent larvae significantly reduce viable conidia by days 5 and 7 postinfection. *, $P < 0.05$ as determined by repeated-measures ANOVA and Tukey's HSD method for multiple-comparison test. (D) At 2 days postinfection, control larvae harbor ungerminated conidia (gray arrows), while macrophage- and neutrophil-deficient pu.1 morphants succumb to invasive *A. fumigatus* (*gpdA::YFP*) growth. Scale bar, 100 μ m.

and PAK, appropriate stock concentrations were adjusted to ensure that there were 1.0×10^8 conidia/ml and that, after mixing with conidia, PAK was at a final optical density (OD) of 0.1. For survival analysis, infected larvae were individually sorted into single wells of a 96-well plate and monitored every 24 h for the duration of the experiment. For conidial viability assays, single infected larvae or pools of 20 infected larvae were homogenized at the time points indicated into 0.1 ml or 1 ml PBS, respectively. Larval tissue was disrupted to release conidia via shear stress in a bead beater at maximum speed, with no beads added, for 10 s, and if necessary, persisting tissue fragments were passed through a sterile 26-gauge needle.

Fluorescence microscopy. For time lapse fluorescence imaging, anesthetized larvae were positioned onto the bottom of a custom-made glass imaging dish with Tricaine and PTU at the concentrations described above with or without 1% low-melting-point agarose, depending on the duration of imaging. Both time lapse and still images were acquired with a laser scanning confocal microscope (Fluoview FV1000; Olympus, PA) using a numerical aperture 20×0.75 objective. During confocal imaging, differential interference contrast (DIC) and fluorescence channels (488 nm and 543 nm) were obtained via sequential line scanning. Z-stack acquisition utilized an 80- μ m pinhole and 10- μ m step sizes.

Statistical analyses. Repeated-measures analysis of variance (ANOVA) was conducted to compare normalized CFU counts between groups for different days postinfection (dpi). Pairwise comparisons between normalized CFU counts between dpi groups were performed using Tukey's honestly significant difference (HSD) method. The data were summarized in graphical format using bar charts with the corresponding error bars. Survival data from at least three independent experimental replicates were pooled and analyzed

using Cox proportional-hazard regression analysis where the experimental conditions were included as group variables. The utilization of the Cox proportional-hazard model for analyzing the survival outcomes allows for this incorporation of several group variables into a comprehensive model. The survival distributions for the different experimental conditions were displayed in graphical format using Kaplan-Meier plots. All P values were two sided, and a P value of < 0.05 was used to define statistical significance. Data analyses were conducted using GraphPad Prism version 6 and R statistical software version 3 (33).

RESULTS

Invasive *A. fumigatus* infection in immunodeficient zebrafish larvae. To determine if immunocompetent zebrafish larvae develop invasive aspergillosis (IA), we performed localized hind-brain ventricle microinjections with *A. fumigatus* conidia at ~32 hpf (Fig. 1A) using modifications of a previously published protocol (18). Immunocompetent (control MO) larvae had ~100% survival at 1 week following infection (Fig. 1B). Previous studies have shown that innate phagocytes can kill *A. fumigatus* conidia over time *in vitro* (34). Therefore, to determine if conidial killing accompanied immunocompetent larval survival *in vivo*, pools of 20 larvae were homogenized at 0, 1, 3, 5, and 7 days postinfection (dpi) to assess the average fungal burden throughout the course of infection. Surprisingly, it was not until 5 and 7 dpi that we found a significant decrease ($P < 0.05$) in viable conidia (Fig. 1C). To rule out the possibility of individual larvae within the pool skew-

ing average CFU counts with particularly high or low burdens, single larvae were homogenized and plated. This approach yielded a similar trend, with a ~60% decrease in CFU by 7 dpi (see Fig. S1 in the supplemental material), indicating that although the infection was controlled, it was not rapidly cleared in immunocompetent larvae.

As IA is a disease largely affecting patients with defects in innate immunity, we next sought to determine whether phagocytes of the innate immune system are responsible for larval survival following challenge with *A. fumigatus*. To test this question, we utilized morpholino-mediated knockdown (21) of pu.1, a transcription factor required for differentiation of myelo-erythroid progenitor cells into the myeloid lineage. The pu.1 morpholino impairs formation of both macrophages and neutrophils in developing larvae (30), which are the primary cells of the innate immune response. pu.1 morphant larvae were highly susceptible ($P < 0.0001$) to wild-type *A. fumigatus* (*gpdA::GFP::his2A*) infection, with ~100% mortality by 3 days postinfection, whereas mock infection caused no host mortality (Fig. 1B). Heat inactivation of conidia abrogated the effects on mortality in pu.1 morphants (Fig. 1B). Additionally, we verified in our model that a known avirulent strain (35, 36) deficient in production of the siderophore precursor L-ornithine- N^5 -monooxygenase (Δ *sidA*) did not cause disease in pu.1 morphant larvae ($P > 0.1$) (Fig. 1B).

To understand why *A. fumigatus* causes lethal infection in pu.1 morphant larvae, we imaged a strain of *A. fumigatus* that constitutively expresses YFP (*gpdA::YFP*) in both control and pu.1 morphants. While hyphal formation was rarely observed in immunocompetent larvae, we found that pu.1 morphants succumb to aggressive hyphal growth and invasive disease (Fig. 1D; see Movie S1 in the supplemental material). Of note, hyphae frequently penetrated into neighboring tissues and at times were seen breaking through the epithelium. Taking these results together, we conclude that *A. fumigatus* causes invasive disease within the larval zebrafish in the absence of innate phagocytes.

Macrophages rapidly phagocytose *A. fumigatus* conidia and mediate host survival. One of the main advantages of the larval zebrafish lies in its optical transparency, allowing direct observation of innate immune responses to *A. fumigatus*. Having already established the importance of innate phagocytes in controlling IA in zebrafish larvae (Fig. 1B), we next wanted to characterize the contributions of individual macrophage and neutrophil populations toward host recognition of and survival against *A. fumigatus*. Since macrophages are known to be critical responders to *A. fumigatus* (37–40), we next used transgenic fish specifically expressing the fluorescent protein Dendra2 in macrophages [*Tg(mpeg1:dendra2)*] (41), facilitating direct observation of macrophage-*A. fumigatus* interactions *in vivo*. For fluorescent contrast, we used an mCherry-expressing strain (42) of *A. fumigatus* (*gpdA::mCherry::his2A*). Immediately following infection, macrophages phagocytosed the majority of conidia within 6 h (Fig. 2A; see Movie S2 in the supplemental material). More clearly visible in Movie S2, we routinely observed a small subset of macrophages (usually on the order of two to five cells) phagocytosing a disproportionately high number of conidia such that the number of fungal cells per macrophage became too numerous to quantify, a behavior reported in murine alveolar macrophages as well (43). Additionally, at up to 7 dpi, it was possible to observe fluorescent conidia within macrophages in tissues beyond the hindbrain, suggesting that macro-

phages containing viable conidia disseminate out of the site of infection (data not shown).

Earlier observations during infection revealed that conidia can, albeit infrequently, germinate into hyphae in immunocompetent larvae. Therefore, we wanted to exploit this opportunity to capture a wild-type host response to *A. fumigatus* hyphae *in vivo*. To this end, large numbers of infected larvae were screened at 1 dpi for hyphae. Whenever hyphae were observed in an immunocompetent host, macrophages were always present. The degree of macrophage inflammation, however, varied from several cells colocalized with hyphae (Fig. 2B) to large aggregates of macrophages in a long-lasting association (see Movie S3 in the supplemental material). The source of germination, whether originating from non-phagocytosed conidia or from within macrophages, remains to be determined.

Since macrophages rapidly phagocytose conidia and persist beyond germination, we hypothesized that macrophages would contribute to host survival. To address the role of macrophages in host defense against *A. fumigatus*, we depleted macrophages using the *irf8* morpholino. *irf8* is a transcription factor that directs the formation of macrophages during primitive myelopoiesis in zebrafish (31). As a consequence, macrophages are depleted in *irf8* morphants for the first 3 days postinfection (dpf), after which macrophages slowly reappear in diminished numbers (see Fig. S2 in the supplemental material). *irf8* morphant larvae were significantly ($P < 0.0001$) more susceptible to *A. fumigatus* (*gpdA::GFP::his2A*) infection, compared to mock PBS infection, with ~70% survival by 7 dpi (Fig. 2C). This defect in survival, however, was not as remarkable as the findings with pu.1 morphants (Fig. 1B), suggesting that neutrophils also contribute to host survival.

Neutrophils respond to *A. fumigatus* hyphae, but not conidia, and mediate host survival. To determine if neutrophils contribute to host survival in response to *A. fumigatus*, we characterized the neutrophil response to infection. Previous findings suggest that neutrophils are major players in host defense against *A. fumigatus* (1); however, neutrophil interactions with *A. fumigatus* in an intact, live vertebrate host have never been reported. Therefore, we used live imaging and the *Tg(mpx:dendra2)* zebrafish line to specifically observe neutrophil interactions with *A. fumigatus* (*gpdA::mCherry::his2A*) *in vivo*. In contrast to macrophages, we were surprised to find that neutrophils did not phagocytose conidia (Fig. 3A; see Movie S4 in the supplemental material). In contrast, it is known that neutrophils in larval zebrafish rapidly respond to and phagocytose many other pathogens, including bacteria (41, 44–46) and yeast of the fungal pathogen *Candida albicans* (18). This raises the possibility that rapid phagocytosis of conidia by macrophages occurs before neutrophil recognition of the fungus. Therefore, we removed macrophages with the *irf8* morpholino to determine if neutrophils would phagocytose conidia in the absence of macrophages. Even in the absence of macrophages, neutrophils did not phagocytose conidia (Fig. 3B; see Movie S5 in the supplemental material). An alternate hypothesis to account for a lack of neutrophil phagocytosis of conidia is that conidia may release an inhibitory factor, as we recently reported with human neutrophils in response to a bioactive conidial metabolite (47). To test this idea, we coinjected conidia with a low dose of *Pseudomonas aeruginosa* (PAK), which functions as a neutrophil attractant in zebrafish larvae (26, 32, 48). With forced neutrophil recruitment to the hindbrain with PAK, we saw a continued lack of conidial phagocytosis by neutrophils

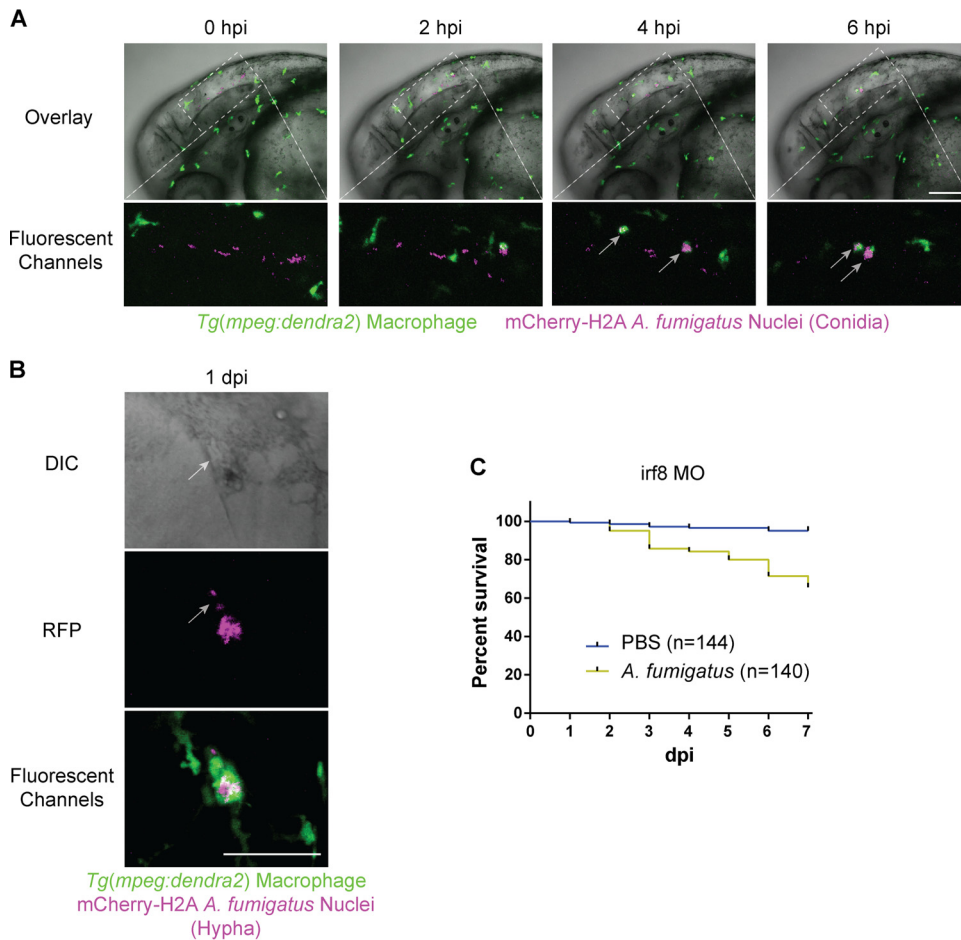


FIG 2 Macrophages phagocytose *A. fumigatus* conidia, colocalize with hyphae, and mediate host survival. (A and B) Immunocompetent larvae with fluorescent macrophages [*Tg(mpeg1:dendra2)*] injected with *A. fumigatus* (*gpdA::mCherry::his2A*). (A) Time lapse imaging immediately following injection shows rapid phagocytosis of conidia by macrophages by 6 hpi (gray arrows) (see also Movie S2 in the supplemental material). Scale bar, 100 μ m. (B) Macrophages closely associate with hyphae in immunocompetent larvae (see also Movie S3 in the supplemental material). Scale bar, 50 μ m. (C) Macrophage-deficient *irf8* morphant larvae exhibit significant ($P < 0.0001$) mortality following challenge with *A. fumigatus* (*gpdA::GFP::his2A*) and not with a mock PBS infection. Survival data are pooled from five independent experimental replicates, and the P value was calculated by Cox proportional-hazard regression analysis.

(Fig. 3C). Taken together, our findings suggest that neutrophils do not phagocytose conidia under the conditions tested.

Collectively, clinical and experimental data show enhanced susceptibility to *Aspergillus* infection in patients with chronic or prolonged neutropenia (1), suggesting a key role for neutrophils in host defense against *Aspergillus*. Additionally, *in vitro* data suggest that neutrophils are particularly responsive to *A. fumigatus* after the fungus has undergone conidial swelling and germination (49–52). We therefore reasoned that zebrafish neutrophils would respond to hyphae *in vivo*. With a rarity of germination in an immunocompetent host, we screened large numbers of larvae infected with *A. fumigatus* at 1 dpi to visualize the wild-type immune response toward hyphae. Neutrophils demonstrated a robust response to hyphae, with rapid migration toward and adhesion to *A. fumigatus* postgermination (Fig. 4A; see Movie S6 in the supplemental material). Movie S6 shows a loss of nuclear fluorescence in the hyphae following adherence of the neutrophil outlined in Fig. 4A (gray arrows), providing evidence for contact-mediated neutrophil killing of hyphae. Follow-up imaging of individual larvae harboring hyphal growth, including the larvae in Fig. 4A and in

Movie S6 (data not shown), revealed that filaments are routinely cleared by 2 dpi (Fig. 4B). This suggests that neutrophils, together with macrophages (Fig. 2B), contribute to host clearance of germinated *A. fumigatus* through fungicidal mechanisms directed at hyphae but not spores.

Given the evidence that neutrophils are present only around tissue-damaging hyphae, we next sought to define the role of neutrophils in host survival against *A. fumigatus*. Previously, our lab generated a transgenic zebrafish line expressing the dominant negative *Rac2*^{D57N} mutation specifically in neutrophils [*Tg(mpx:mCherry-2A-Rac2D57N)*] (D57N) to model a human form of a leukocyte adhesion deficiency (32). *Rac2* belongs to the Rho family of GTPases and plays a role in regulating neutrophil migration and the generation of reactive oxygen species. The inhibitory *Rac2*^{D57N} mutation was originally discovered from a clinical observation of a patient with recurrent infections (53). In zebrafish, the *Rac2*^{D57N} mutation recapitulates a leukocyte adhesion deficiency phenotype such that neutrophils are unable to migrate or properly egress from the circulation, effectively abolishing neutrophil recruitment to infection or tissue damage, resulting in lar-

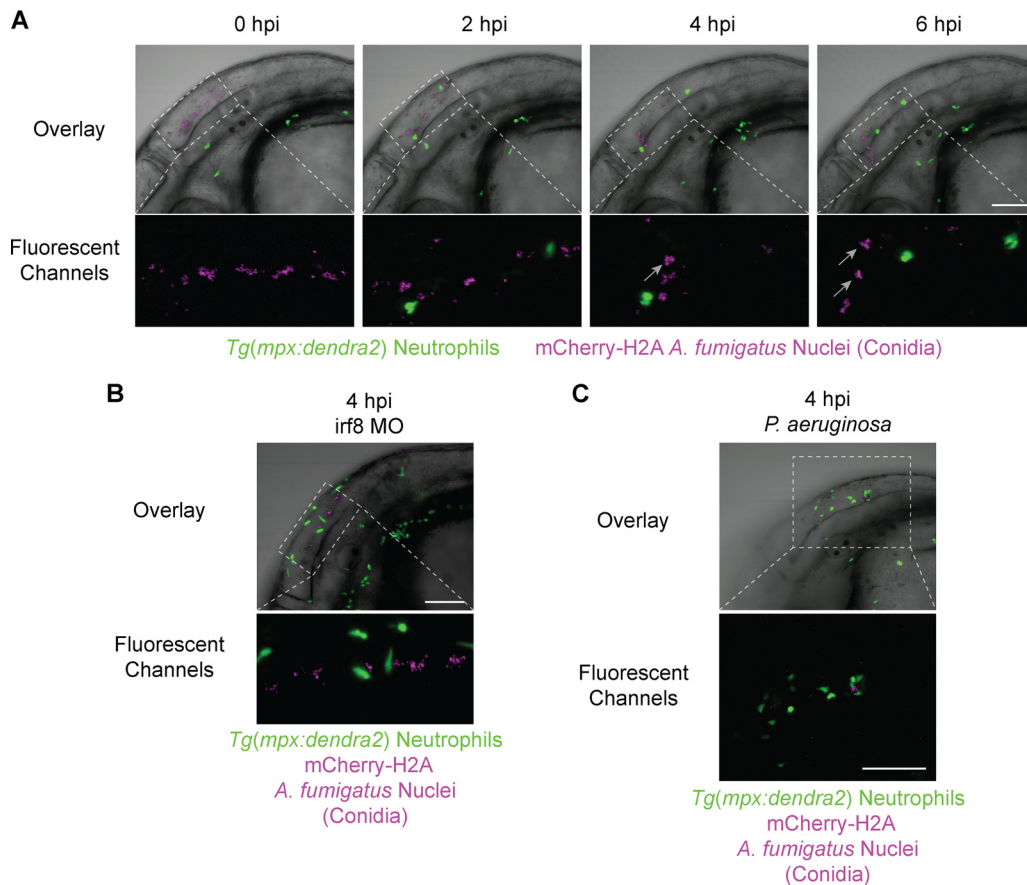


FIG 3 Neutrophils do not phagocytose *A. fumigatus* conidia. Immunocompetent larvae with fluorescent neutrophils [*Tg(mpx:dendra2)*] were injected with *A. fumigatus* (*gpdA::mCherry::his2A*). (A) Time lapse imaging immediately following infection shows a lack of conidial phagocytosis by neutrophils (see also Movie S4 in the supplemental material). Gray arrows indicate conidial clumping resulting from macrophage phagocytosis. (B) Removal of macrophages with the *irf8* morpholino (*irf8* MO) leaves conidia in the extracellular space in the absence of macrophage phagocytosis (see gray arrows in panel A), and neutrophils remain nonphagocytic toward conidia (see also Movie S5 in the supplemental material). (C) Stimulated neutrophil recruitment with *P. aeruginosa* in a coinjection with *A. fumigatus* shows a continued lack of neutrophil phagocytosis of conidia. All images are representative of more than three experimental replicates. Scale bar, 100 μ m.

val susceptibility to bacterial pathogens (32, 41). Here, we used the D57N line to assess host survival against *A. fumigatus* in a neutrophil-deficient background and found that the larvae were highly susceptible ($P < 0.001$) to infection, with 50% mortality by 7 dpi (Fig. 4C), illustrating a key role for neutrophils in host survival against *A. fumigatus*.

Depletion of macrophages, but not loss of neutrophil function, is associated with virulence attenuation of a Δ laeA strain of *A. fumigatus*. We next sought to determine how phagocytes contribute to host defense against a metabolic mutant of *A. fumigatus*. The methyltransferase *LaeA* is a global regulator of fungal metabolism and spore development (29). Null mutants (Δ laeA) of all pathogenic fungal species investigated to date have shown *LaeA* to be an important virulence determinant, in part due to decreased toxin production (54–57). In vertebrates, virulence of *A. fumigatus* Δ laeA has been investigated only in broadly immunosuppressed mice either with cortisone acetate (58) or with both cortisone acetate and cyclophosphamide (54), potentially confounding unique contributions of different innate immune cell types to the host response. Therefore, we wanted to investigate the virulence of an *A. fumigatus* Δ laeA strain (*pyrG*⁻; Δ laeA::*A. para-*

siticus pyrG) in precise immunosuppressed host backgrounds. No attenuation in virulence was observed for the Δ laeA strain in highly immunosuppressed pu.1 larvae (data not shown). To test the role of macrophages in host defense to the Δ laeA strain, we infected macrophage-deficient *irf8* morphants and observed a virulence defect ($P = 0.00027$) with the Δ laeA strain compared to an isogenic complement control (*pyrG*⁻; *A. parasiticus pyrG*), with ~40% and ~60% mortality by 7 dpi, respectively (Fig. 5A). To examine the role of neutrophils, we tested host survival in transgenic D57N larvae and found no difference in virulence ($P = 0.23$) between the Δ laeA and control strains (Fig. 5B). While the wild-type virulence of *A. fumigatus* in Fig. 5A and B is somewhat greater than what was observed in Fig. 2C and 4C, the trend is the same (i.e., greater mortality in D57N larvae than *irf8* morphants), and the appropriate isogenic control was used in parallel to the Δ laeA strain. We did not determine whether there is a difference in virulence between these two “wild-type” strains. We hypothesized that early interactions between Δ laeA conidia and remaining neutrophils in *irf8* morphants may contribute to the *irf8* morphant-specific virulence defect for the Δ laeA strain, especially since Δ laeA conidia are known to have less of the pathogen-associated

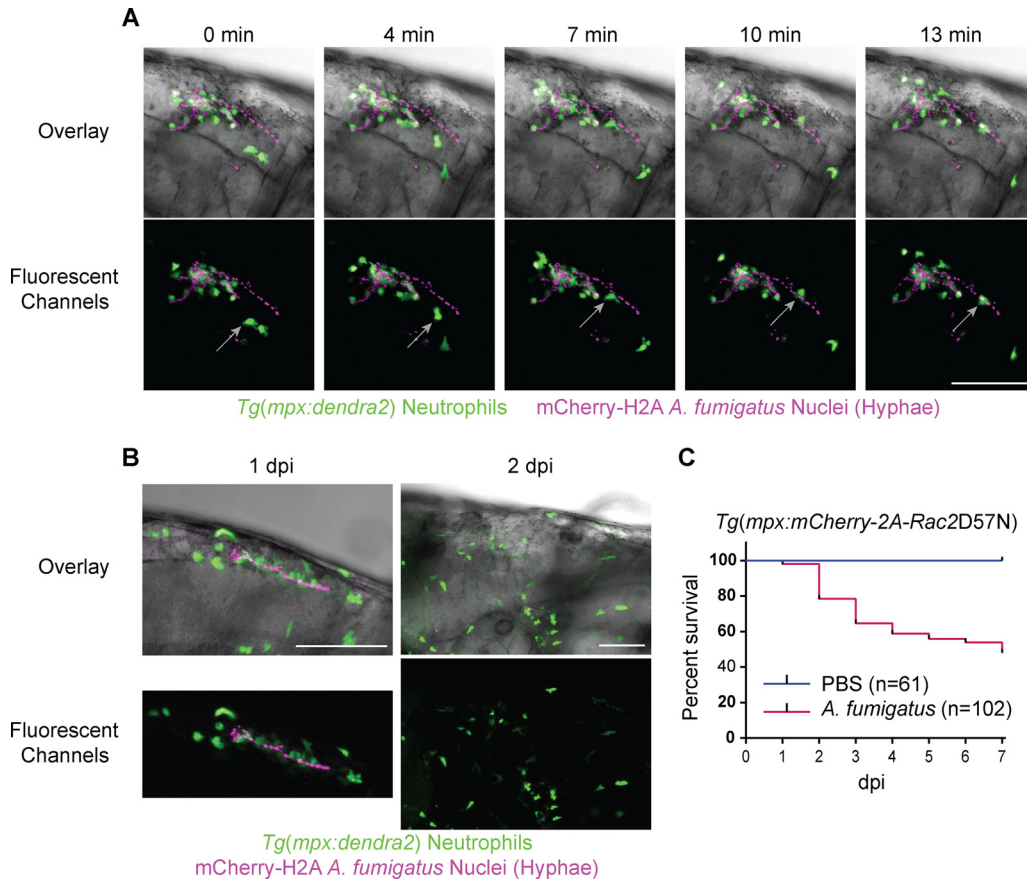


FIG 4 Neutrophils respond to *A. fumigatus* hyphae and mediate host survival. (A and B) Immunocompetent larvae with fluorescent neutrophils [*Tg(mpx:dendra2)*] injected with *A. fumigatus* (*gpdA::mCherry::his2A*) and screened at 1 day postinfection (dpi) for the presence of hyphae. (A) Time lapse imaging reveals a persistent neutrophil response around *A. fumigatus* hyphae characterized by both tight colocalization with the mycelium and migration toward and adherence to hyphal filaments (gray arrow) by individual neutrophils (see also Movie S6 in the supplemental material). (B) Representative images from daily imaging of hypha-containing fish demonstrate host clearance of hyphae at 2 dpi. (C) Larvae expressing the inhibitory Rac2D57N mutation specifically in neutrophils [*Tg(mpx:mCherry-2A-Rac2D57N)*] are highly susceptible ($P < 0.001$) to *A. fumigatus* (*gpdA::GFP::his2A*) infection. Survival data were pooled from five independent experimental replicates, and the P value was calculated by Cox proportional-hazard regression analysis. Scale bar, 100 μ m.

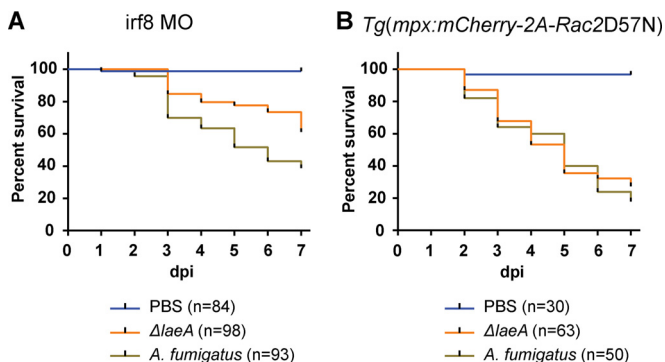


FIG 5 Virulence of *A. fumigatus* $\Delta laeA$ is attenuated only in a macrophage-deficient host. (A) In macrophage-deficient *irf8* morphant larvae, the $\Delta laeA$ strain of *A. fumigatus* (*pyrG*⁻; $\Delta laeA$::*A. parasiticus pyrG*) is significantly less virulent ($P = 0.00027$) than a complement control (*pyrG*⁻; *A. parasiticus pyrG*). (B) Virulence attenuation is not observed ($P = 0.772$) with *A. fumigatus* $\Delta laeA$ in larvae with impaired neutrophil function [*Tg(mpx:mCherry-2A-Rac2D57N)*]. Survival data were pooled from three independent experimental replicates except for the PBS condition in Rac2^{D57N}, which was included in two of the three replicates, and P values were calculated by Cox proportional-hazard regression analysis.

molecular pattern (PAMP)-shielding hydrophobic rodlet layer (59). Time lapse imaging in *irf8* morphant larvae with mCherry-expressing neutrophils [*Tg(mpx:mCherry)*] and a GFP-expressing $\Delta laeA$ strain showed no neutrophil phagocytosis of $\Delta laeA$ conidia (see Movie S7 in the supplemental material). This suggests that interactions between the $\Delta laeA$ strain and neutrophils occur later in infection. It is possible that postgermination events involving the production of numerous toxic hyphal secondary metabolites (54, 60) may be responsible for the observed virulence attenuation in macrophage-deficient larvae.

DISCUSSION

Here, we exploited the larval zebrafish as an infection host to study the innate immune response to the opportunistic human pathogen *A. fumigatus*. Our study highlights the advantages of live imaging in zebrafish to study invasive growth of *A. fumigatus* and the innate immune response to different developmental stages of the fungus. Moreover, by employing zebrafish with specific immune deficiencies, we were able to dissect the roles of neutrophils and macrophages in innate immunity against *A. fumigatus*. The discovery that neutrophils are critical for the differential virulence of an *A. fumigatus* secondary metabolite mutant supports the sensi-

tivity of this model to dissect fungal mechanisms and the cell biology of the host response.

We found that like in humans and mice, invasive disease occurred at a very low frequency in wild-type zebrafish larvae, suggesting that larvae possess an effective innate host defense against *A. fumigatus*. It is intriguing, however, that conidia persist with only an ~60% reduction in fungal burden by 7 dpi, despite the absence of apparent infection; this provides insight as to how persistence of conidia may subsequently lead to invasive disease. Previous research has shown that the conidial pigment and structural surface molecule dihydroxynaphthalene (DHN)-melanin of *A. fumigatus* provides resistance to oxidative stress (61), inhibits phagolysosome acidification (39, 62, 63), and modulates the host cytokine response (64). For future studies, it will be interesting to determine whether DHN-melanin contributes to the persistence phenotype observed *in vivo* in zebrafish. Additionally, the hydrophobic coating of conidia with the RodA protein, which has been shown to mask fungal PAMPs and largely render dormant conidia immunologically inert (65), may also be playing a role in inhibiting host recognition, and full host clearance, of conidia.

Until now, it has not been possible to exclusively analyze interactions between phagocytes of innate immunity and *A. fumigatus* in a live vertebrate model host of IA. While studies of innate immunity using murine models can benefit from precise cell type-specific knockdown of neutrophils and macrophages via monoclonal antibodies and clodronate liposomes, respectively (12), nontargeted elements of innate and adaptive immunity (13) that are known to play a role in modulating host responses to *A. fumigatus* may continue to influence experimental outcomes. With adaptive immunity not reaching functional maturity in the larval zebrafish until several weeks postfertilization (14, 66, 67), the larval model of IA provides an ideal vertebrate environment for unbiased *in vivo* study of innate responses to *A. fumigatus*. To probe innate immunity, we first utilized morpholino-mediated knockdown of the transcription factor pu.1, which during early myelopoiesis directs differentiation of myelo-erythroid progenitor cells into the myeloid lineage (30), rendering larvae severely immunocompromised and devoid of both macrophages and neutrophils. While pu.1 morphants have been adopted for the study of myeloid cell contributions toward host protection against disease from bacterial pathogens (26, 41, 46, 68, 69), to date they have not been applied to study fungal virulence. With pu.1 morphants, we showed that innate phagocytes are essential for controlling *A. fumigatus* infection, with nearly 100% mortality by 3 dpi, which is in agreement with the rapid mortality observed in broadly immunosuppressed murine models of IA (35, 54, 70). Mortality was accompanied by extensive hyphal growth and penetration into adjacent tissues, which are a defining hallmark of IA. The extent of hyphal growth and invasive behavior, most notably epithelial extrusion of hyphae, provides a tool to further understand the cell biology of epithelial cell responses to hyphae.

pu.1 morphants are highly susceptible to other pathogens, and only a nonpathogenic strain of *Escherichia coli* does not result in host mortality (68). To validate the model, we show that the nonpathogenic *A. fumigatus* Δ *sidA* strain is avirulent in pu.1 morphants. *sidA* is required for siderophore biosynthesis and iron acquisition, and loss of this protein renders the fungus avirulent in murine models as well (35, 36). Additionally, *A. fumigatus* has been shown to be susceptible to human neutrophil-mediated iron depletion *in vitro* (71), supporting the idea that like other verte-

brates (72), zebrafish larvae may restrict the availability of essential nutrients, such as iron, as a means of defense against pathogens.

In humans and other vertebrate models of IA, it is widely accepted that resident pulmonary macrophages represent the first line of defense against inhaled conidia (1, 73, 74). With extensive functional parallels between zebrafish and mammalian macrophages (17, 75), we were eager to visualize macrophage interactions with *A. fumigatus* in a live vertebrate host. Following challenge with *A. fumigatus*, we provide real-time *in vivo* evidence that macrophages efficiently phagocytose conidia. While dormant conidia can largely be considered immunologically inert due to their PAMP-masking surface structures (65), the exact mechanisms underlying macrophage phagocytosis of resting conidia are still unknown but are likely mediated by c-type lectins as well as Toll-like receptor 2 (TLR2) and the adaptor molecule Myd88 (76). Interestingly, while numerous macrophages are present in the hindbrain following injection, the majority of conidia are phagocytosed by a small subset of macrophages, possibly from a specific population of resident macrophages. This behavior has been observed in murine macrophages as well (43), suggesting a conserved pattern of phagocytosis among vertebrate macrophages.

While infrequent, germination can occur in immunocompetent larvae. Therefore, we used these events to observe macrophage-hyphal interactions in wild-type larvae and found that macrophages formed dense aggregates around hyphae, indicating that macrophages respond to all stages of *A. fumigatus* morphological development. We cannot rule out the possibility that these observed germination events in immunocompetent larvae are due to naturally occurring genetic variations that may alter immune function and contribute to susceptibility. Because of a scarcity of germination in immunocompetent larvae, we were unable to determine if germination occurred within macrophages, an interesting area for future investigation. Evidence suggests that *A. fumigatus* can germinate postphagocytosis and lyse macrophages *in vitro* (34). While our images (not shown) of early germlings appeared to support this, we cannot conclude that this is occurring *in vivo* because we were unable to capture macrophage membrane lysis with time lapse imaging. Additionally, it could be argued that we witnessed partial hyphal phagocytosis by macrophages, which has been documented *in vitro* (38). Similar to *A. fumigatus*, *in vitro* studies with the dimorphic fungal pathogen *C. albicans* show penetrating hyphal growth from within phagocytes (77). Similarly, using a larval zebrafish model, Brothers et al. (18) were unable to capture *C. albicans* phagocyte escape in a live host. Despite the potential clinical significance, it is still unclear whether or not this *in vitro/in vivo* discrepancy of phagocyte escape exists for *A. fumigatus*.

Since macrophages are present around all morphological states of *A. fumigatus* from spores to hyphae in infected larvae, we expected to see more severe host mortality than what was experimentally observed in macrophage-deficient *irf8* morphants. These findings may help to reconcile conflicting conclusions in the field about the protective roles of macrophages against *A. fumigatus*. For example, with clodronate liposome-mediated macrophage depletion in mice, Mircescu et al. (12) concluded that macrophages are dispensable for inhibiting germination and host survival, while Bhatia et al. (37) reported a protective role for macrophages after showing an increased fungal burden in the absence of macrophages. Our findings, from a model completely

dependent on innate immune defenses, indicate that macrophages do in fact contribute to host survival.

Early evidence suggested that neutrophils are the dominant phagocyte against hyphae (40). While a number of studies challenged this idea after showing *in vivo* neutrophil infiltration to the murine lung following concentrated conidial dosage (43, 50), other findings show that excessive IA-induced neutrophilic inflammation in the lungs of mice undergoing corticosteroid treatment is frequently the major feature under these conditions (8). These findings highlight a critical role for balanced neutrophil participation in the removal of *A. fumigatus*. However, in contrast to *in vitro* reports of neutrophil phagocytosis of conidia (51, 63), our findings demonstrate a nearly complete lack of conidial phagocytosis by neutrophils *in vivo*. Furthermore, our observed absence of conidial phagocytosis by neutrophils may be specific to *A. fumigatus* and not represent a general response toward fungi, because in a similar larval zebrafish infection model (18), neutrophils were seen phagocytosing yeast cells of *C. albicans*.

We found that addition of *P. aeruginosa* did not impact neutrophil phagocytosis of *A. fumigatus* conidia. It has been shown previously that *A. fumigatus* conidia possess endocrocin, a secondary metabolite with neutrophil chemotaxis-inhibiting properties (47). Endocrocin biosynthesis is temperature dependent with increased production at 25°C compared to 37°C during sporulation (47, 78). Given that virtually all studies addressing *A. fumigatus* virulence grow the fungus at 37°C prior to harvesting spores, we chose to do so in this initial study for reasons of consistency. Thus, the conidia in this study had little to no endocrocin. Therefore, it is unlikely that endocrocin is responsible for the lack of neutrophil recruitment to conidia. Future studies of *A. fumigatus* virulence in zebrafish larvae will have to consider the reduced infection temperature compared to that in mammalian models. However, temperature-associated genes characterized thus far in *A. fumigatus* have yet to provide a direct link between specific thermally regulated genes and virulence (79, 80). Another factor that may be contributing to our observed lack of conidial phagocytosis by neutrophils is that neutrophils can exhibit distinct tissue-dependent phagocytic behaviors. For example, it was shown in zebrafish larvae that neutrophils have paltry phagocytic behavior toward *E. coli* in fluid-filled spaces, such as the hindbrain, while assuming the dominant phagocytic role in surface-associated bacteria (45).

Neutrophil phagocytosis of bacterial pathogens, such as PAK, has been well documented in zebrafish larvae (41, 48). Regardless of whether macrophages were present or absent or whether neutrophils were artificially recruited to the hindbrain with *P. aeruginosa* to force tight spatial interactions with the fungus, neutrophils did not phagocytose conidia. At this point we cannot exclude the possibility of PAK modulating the phagocytic response or of complex polymicrobial interactions influencing neutrophil behavior toward conidia.

In sharp contrast to neutrophil behavior toward conidia, whenever hyphal growth appeared in immunocompetent larvae, we found that neutrophils robustly migrated toward and adhered to the mycelium. Additionally, Movie S6 in the supplemental material in its entirety shows a diminution of histone red fluorescent protein (RFP) fluorescence in the hypha following neutrophil attachment. This leads us to speculate that localized loss of hyphal fluorescence was due to contact-dependent fungicidal mechanisms from the neutrophil, such as degranulation or neutrophil

extracellular trap (NET) formation. Hyphae have been shown to be potent stimulators of neutrophil degranulation (51, 71) and of NET formation in both *in vitro* and *in vivo* systems (49). Possibly contributing to neutrophil recognition of hyphae is the exposure of fungal PAMPs on the hyphal surface, which are masked on dormant conidia by the hydrophobic layer composed of the protein RodA and the structural pigment DHN-melanin. Removal of RodA through conidial swelling and germination has been shown to elicit a much stronger immune response over dormant conidia (49, 50, 65, 81). Even though macrophages are not labeled in our neutrophil images, we have shown that they too are present around hyphae, suggesting an organized fungicidal effort between both phagocyte populations against hyphae.

Following the observation of neutrophil attacks on hyphal filaments, we wanted to determine the extent to which neutrophils contribute to host survival against *A. fumigatus*. To address this question, we utilized a transgenic zebrafish line expressing the dominant negative Rac2^{D57N} mutation specifically in neutrophils (32). Following infection with *A. fumigatus*, transgenic Rac2^{D57N} larvae were susceptible to lethal infection, with mortality reaching up to 50% by 7 dpi. Additionally, Deng et al. (32) reported functional recapitulation of neutrophil deficiencies observed in the D57N line in larvae injected with the Rac2 morpholino. We observed a similar survival outcome (50% mortality by day 7) in Rac2 morphant larvae compared to transgenic Rac2^{D57N} larvae under identical infection conditions (data not shown). This suggests that, even with stochastic dilution of morpholinos resulting from developing larvae and diminution of the morpholino concentration over time (21, 82), once hyphae are able to establish penetrative growth, host clearance of the infection is difficult.

Through the use of precise genetic manipulation available in zebrafish larvae we were able to show, for the first time, an immunosuppression-specific virulence attenuation of a $\Delta laeA$ strain of *A. fumigatus*. The LaeA protein is a methyltransferase (83) conserved throughout ascomycete fungi and is known for its role in global regulation of fungal secondary metabolism (29, 84). However, additional evidence is surfacing linking LaeA-mediated regulation of primary metabolic processes as well, such as iron (85) and sulfur (S. Jain and N. P. Keller, unpublished data) metabolism. As a consequence, pinpointing the exact causes of LaeA-mediated virulence determinants becomes difficult given the pleiotropic nature of this protein. Previously, using different murine models of IA, it was shown that an *A. fumigatus* $\Delta laeA$ strain was less virulent (54, 58). While effective in showing that LaeA contributes to *A. fumigatus* virulence, these studies used broadly immunosuppressed mice, thereby masking any unique contributions to host defense from particular phagocytes of the innate immune system. Larval zebrafish, on the other hand, which are completely dependent upon innate immunity, allowed us to determine that the $\Delta laeA$ strain was attenuated in virulence only in the absence of macrophages (irf8 MO) and not in the absence of functional neutrophils (D57N), suggesting that loss of LaeA renders the fungus susceptible primarily to neutrophil attack. We investigated whether or not $\Delta laeA$ conidia attracted neutrophils in irf8 morphant larvae, which could have accounted for the attenuation phenotype, and found there to be no $\Delta laeA$ conidial phagocytosis by neutrophils within 8 hpi. As a result, enhanced neutrophil-mediated killing of the $\Delta laeA$ strain is potentially occurring later in infection, possibly at the hyphal stage, which may correlate with production of hypha-specific toxins or activation of nutrient

scavenging programs (85). In any case, these findings support the essential role for neutrophils, more than macrophages, in defense against this particular attenuated strain of *A. fumigatus*.

Taken together, our data show an organized innate immune response dependent upon the morphological state of *A. fumigatus* such that macrophages rapidly phagocytose conidia and persist around hyphae while neutrophils respond only to the hyphal form. When functioning properly, this stage-specific arrangement effectively prevents invasive infection, likely via the rapid sequestering of conidia within macrophages, while delaying the potentially damaging effects of neutrophil inflammation to host tissue unless absolutely necessary to combat invasive hyphal growth. With precise genetic tools widely accessible on both the host and pathogen sides, this model will allow for further characterization of the molecular mechanisms that dictate *Aspergillus*-phagocyte interactions and provide a visual platform for rapid screening and drug testing studies. A challenge for future investigation will be to determine specific factors on both the host and fungal sides that control fungal killing and persistence, respectively, and how this balance may be shifted by immunologic risk factors and therapeutics.

ACKNOWLEDGMENTS

We thank Wen-Bing Yin, Jonathan Palmer, and Sven Krappmann for providing strains of *A. fumigatus* (see Table S1 in the supplemental material), members of the Huttenlocher laboratory for zebrafish care and maintenance, and members of both the Keller and Huttenlocher laboratories for spirited discussions.

This work was supported by the National Science Foundation-Emerging Frontiers in Research and Innovation-MIKS (grant 1136903 to A.H. and N.P.K.).

REFERENCES

- Latgé J. 1999. *Aspergillus fumigatus* and Aspergillosis. *Clin. Microbiol. Rev.* 12:310–350.
- Roilides E, Holmes A, Blake C, Pizzo PA, Walsh TJ. 1993. Impairment of neutrophil antifungal activity against hyphae of *Aspergillus fumigatus* in children infected with human immunodeficiency virus. *J. Infect. Dis.* 167:905–911. <http://dx.doi.org/10.1093/infdis/167.4.905>.
- Roilides E, Holmes A, Blake C, Pizzo PA, Walsh TJ. 1993. Defective antifungal activity of monocyte-derived macrophages from human immunodeficiency virus-infected children against *Aspergillus fumigatus*. *J. Infect. Dis.* 168:1562–1565. <http://dx.doi.org/10.1093/infdis/168.6.1562>.
- Denning DW. 1998. Invasive aspergillosis. *Clin. Infect. Dis.* 26:781–805. <http://dx.doi.org/10.1086/513943>.
- Marr KA, Carter RA, Boeckh M, Martin P, Corey L. 2002. Invasive aspergillosis in allogeneic stem cell transplant recipients: changes in epidemiology and risk factors. *Blood* 100:4358–4366. <http://dx.doi.org/10.1182/blood-2002-05-1496>.
- Hope WW, Walsh TJ, Denning DW. 2005. Laboratory diagnosis of invasive aspergillosis. *Lancet Infect. Dis.* 5:609–622. [http://dx.doi.org/10.1016/S1473-3099\(05\)70238-3](http://dx.doi.org/10.1016/S1473-3099(05)70238-3).
- Marr KA, Boeckh M, Carter RA, Kim HW, Corey L. 2004. Combination antifungal therapy for invasive aspergillosis. *Clin. Infect. Dis.* 39:797–802. <http://dx.doi.org/10.1086/423380>.
- Balloy V, Huerre M, Latgé J, Chignard M. 2005. Differences in patterns of infection and inflammation for corticosteroid treatment and chemotherapy in experimental invasive pulmonary aspergillosis. *Infect. Immun.* 73:494–503. <http://dx.doi.org/10.1128/IAI.73.1.494-503.2005>.
- Chamilos G, Luna M, Lewis RE, Bodey GP, Chemaly R, Tarrand JJ, Safdar A, Raad II, Kontoyiannis DP. 2006. Invasive fungal infections in patients with hematologic malignancies in a tertiary care cancer center: an autopsy study over a 15-year period (1989–2003). *Haematologica* 91:986–989.
- Lionakis MS, Kontoyiannis DP. 2003. Glucocorticoids and invasive fungal infections. *Lancet* 362:1828–1838. [http://dx.doi.org/10.1016/S0140-6736\(03\)14904-5](http://dx.doi.org/10.1016/S0140-6736(03)14904-5).
- Stephens-Romero SD, Mednick AJ, Feldmesser M. 2005. The pathogenesis of fatal outcome in murine pulmonary aspergillosis depends on the neutrophil depletion strategy. *Infect. Immun.* 73:114–125. <http://dx.doi.org/10.1128/IAI.73.1.114-125.2005>.
- Mircescu MM, Lipuma L, van Rooijen N, Pamer EG, Hohl TM. 2009. Essential role for neutrophils but not alveolar macrophages at early time points following *Aspergillus fumigatus* infection. *J. Infect. Dis.* 200:647–656. <http://dx.doi.org/10.1086/600380>.
- Bozza S, Gaziano R, Spreca A, Bacci A, Montagnoli C, di Francesco P, Romani L. 2002. Dendritic cells transport conidia and hyphae of *Aspergillus fumigatus* from the airways to the draining lymph nodes and initiate disparate Th responses to the fungus. *J. Immunol.* 168:1362–1371. <http://dx.doi.org/10.4049/jimmunol.168.3.1362>.
- Lam S, Chua H, Gong Z, Lam T, Sin Y. 2004. Development and maturation of the immune system in zebrafish, *Danio rerio*: a gene expression profiling, in situ hybridization and immunological study. *Dev. Comp. Immunol.* 28:9–28. [http://dx.doi.org/10.1016/S0145-305X\(03\)00103-4](http://dx.doi.org/10.1016/S0145-305X(03)00103-4).
- Van der Vaart M, Spaik HP, Meijer AH. 2012. Pathogen recognition and activation of the innate immune response in zebrafish. *Adv. Hematol.* 2012:159807. <http://dx.doi.org/10.1155/2012/159807>.
- Stockhammer OW, Zakrzewska A, Hegedüs Z, Spaik HP, Meijer AH. 2009. Transcriptome profiling and functional analyses of the zebrafish embryonic innate immune response to *Salmonella* infection. *J. Immunol.* 182:5641–5653. <http://dx.doi.org/10.4049/jimmunol.0900082>.
- Meeker ND, Trede NS. 2008. Immunology and zebrafish: spawning new models of human disease. *Dev. Comp. Immunol.* 32:745–757. <http://dx.doi.org/10.1016/j.dci.2007.11.011>.
- Brothers KM, Newman ZR, Wheeler RT. 2011. Live imaging of disseminated candidiasis in zebrafish reveals role of phagocyte oxidase in limiting filamentous growth. *Eukaryot. Cell* 10:932–944. <http://dx.doi.org/10.1128/EC.05005-11>.
- Brothers KM, Gratacap RL, Barker SE, Newman ZR, Norum A, Wheeler RT. 2013. NADPH oxidase-driven phagocyte recruitment controls *Candida albicans* filamentous growth and prevents mortality. *PLoS Pathog.* 9:e1003634. <http://dx.doi.org/10.1371/journal.ppat.1003634>.
- Gratacap RL, Rawls JF, Wheeler RT. 2013. Mucosal candidiasis elicits NF- κ B activation, proinflammatory gene expression and localized neutrophilia in zebrafish. *Dis. Model. Mech.* 6:1260–1270. <http://dx.doi.org/10.1242/dmm.012039>.
- Nasevicius A, Ekker SC. 2000. Effective targeted gene “knockdown” in zebrafish. *Nat. Genet.* 26:216–220. <http://dx.doi.org/10.1038/79951>.
- Bedell VM, Wang Y, Campbell JM, Poshusta TL, Starker CG, Krug RG, Tan W, Penheiter SG, Ma AC, Leung AYH, Fahrenkrug SC, Carlson DF, Voytas DF, Clark KJ, Essner JJ, Ekker SC. 2012. In vivo genome editing using a high-efficiency TALEN system. *Nature* 491:114–118. <http://dx.doi.org/10.1038/nature11537>.
- Tobin DM, Vary JC, Ray JP, Walsh GS, Dunstan SJ, Bang ND, Hagge DA, Khadge S, King M-C, Hawn TR, Moens CB, Ramakrishnan L. 2010. The *Ita4h* locus modulates susceptibility to mycobacterial infection in zebrafish and humans. *Cell* 140:717–730. <http://dx.doi.org/10.1016/j.cell.2010.02.013>.
- Yoo SK, Huttenlocher A. 2011. Spatiotemporal photolabeling of neutrophil trafficking during inflammation in live zebrafish. *J. Leukoc. Biol.* 89:661–667. <http://dx.doi.org/10.1189/jlb.1010567>.
- Shimizu K, Keller NP. 2001. Genetic involvement of a cAMP-dependent protein kinase in a G protein signaling pathway regulating morphological and chemical transitions in *Aspergillus nidulans*. *Genetics* 157:591–600.
- Brannon MK, Davis JM, Mathias JR, Hall CJ, Emerson JC, Crosier PS, Huttenlocher A, Ramakrishnan L, Moskowitz SM. 2009. *Pseudomonas aeruginosa* type III secretion system interacts with phagocytes to modulate systemic infection of zebrafish embryos. *Cell. Microbiol.* 11:755–768. <http://dx.doi.org/10.1111/j.1462-5822.2009.01288.x>.
- Keller NP, Turner G. 2012. Fungal secondary metabolism: methods and protocols. Humana Press, Totowa, NJ.
- Yu J-H, Hamari Z, Han K-H, Seo J-A, Reyes-Domínguez Y, Sczaccocchio C. 2004. Double-joint PCR: a PCR-based molecular tool for gene manipulations in filamentous fungi. *Fungal Genet. Biol.* 41:973–981. <http://dx.doi.org/10.1016/j.fgb.2004.08.001>.
- Bok JW, Keller NP. 2004. *LaeA*, a regulator of secondary metabolism in *Aspergillus* spp. *Eukaryot. Cell* 3:527–535. <http://dx.doi.org/10.1128/EC.3.2.527-535.2004>.
- Rhodes J, Hagen A, Hsu K, Deng M, Liu TX, Look A, Kanki TJP. 2005.

- Interplay of pu.1 and gata1 determines myelo-erythroid progenitor cell fate in zebrafish. *Dev. Cell* 8:97–108. <http://dx.doi.org/10.1016/j.devcel.2004.11.014>.
31. Li L, Jin H, Xu J, Shi Y, Wen Z. 2011. Irf8 regulates macrophage versus neutrophil fate during zebrafish primitive myelopoiesis. *Blood* 117:1359–1369. <http://dx.doi.org/10.1182/blood-2010-06-290700>.
 32. Deng Q, Yoo SK, Cavnar PJ, Green JM, Huttenlocher A. 2011. Dual roles for Rac2 in neutrophil motility and active retention in zebrafish hematopoietic tissue. *Dev. Cell* 21:735–745. <http://dx.doi.org/10.1016/j.devcel.2011.07.013>.
 33. R Development Core Team. 2013. R: a language and environment for statistical computing. R Foundation for Statistical Computing.
 34. Slesiona S, Gressler M, Mihlan M, Zaehle C, Schaller M, Barz D, Hube B, Jacobsen ID, Brock M. 2012. Persistence versus escape: *Aspergillus terreus* and *Aspergillus fumigatus* employ different strategies during interactions with macrophages. *PLoS One* 7:e31223. <http://dx.doi.org/10.1371/journal.pone.0031223>.
 35. Schrettl M, Bignell E, Kragl C, Joehel C, Rogers T, Arst HN, Haynes K, Haas H. 2004. Siderophore biosynthesis but not reductive iron assimilation is essential for *Aspergillus fumigatus* virulence. *J. Exp. Med.* 200:1213–1219. <http://dx.doi.org/10.1084/jem.20041242>.
 36. Hissen AHT, Wan ANC, Warwas ML, Pinto LJ, Moore MM. 2005. The *Aspergillus fumigatus* siderophore biosynthetic gene sidA, encoding L-ornithine N 5-oxygenase, is required for virulence. *Infect. Immun.* 73:5493–5503. <http://dx.doi.org/10.1128/IAI.73.9.5493-5503.2005>.
 37. Bhatia S, Fei M, Yarlagadda M, Qi Z, Akira S, Saijo S, Iwakura Y, van Rooijen N, Gibson GA, St Croix CM, Ray A, Ray P. 2011. Rapid host defense against *Aspergillus fumigatus* involves alveolar macrophages with a predominance of alternatively activated phenotype. *PLoS One* 6:e15943. <http://dx.doi.org/10.1371/journal.pone.0015943>.
 38. Gersuk GM, Underhill DM, Zhu L, Marr KA. 2006. Dectin-1 and TLRs permit macrophages to distinguish between different *Aspergillus fumigatus* cellular states. *J. Immunol.* 176:3717–3724. <http://dx.doi.org/10.4049/jimmunol.176.6.3717>.
 39. Ibrahim-Granet O, Philippe B, Boleti H, Boisvieux-Ulrich E, Grenet D, Stern M, Latgé JP. 2003. Phagocytosis and intracellular fate of *Aspergillus fumigatus* conidia in alveolar macrophages. *Infect. Immun.* 71:891–903. <http://dx.doi.org/10.1128/IAI.71.2.891-903.2003>.
 40. Schaffner A, Douglas H, Braude A. 1982. Selective protection against conidia by mononuclear and against mycelia by polymorphonuclear phagocytes in resistance to *Aspergillus*: observations on these two lines of defense in vivo and in vitro with human and mouse phagocytes. *J. Clin. Invest.* 69:617–631. <http://dx.doi.org/10.1172/JCI110489>.
 41. Harvie EA, Green JM, Neely MN, Huttenlocher A. 2013. Innate immune response to *Streptococcus iniae* infection in zebrafish larvae. *Infect. Immun.* 81:110–121. <http://dx.doi.org/10.1128/IAI.00642-12>.
 42. Szewczyk E, Krappmann S. 2010. Conserved regulators of mating are essential for *Aspergillus fumigatus* cleistothecium formation. *Eukaryot. Cell* 9:774–783. <http://dx.doi.org/10.1128/EC.00375-09>.
 43. Bonnett CR, Cornish EJ, Harmsen AG, Burritt JB. 2006. Early neutrophil recruitment and aggregation in the murine lung inhibit germination of *Aspergillus fumigatus* conidia. *Infect. Immun.* 74:6528–6539. <http://dx.doi.org/10.1128/IAI.00909-06>.
 44. Deng Q, Harvie EA, Huttenlocher A. 2012. Distinct signalling mechanisms mediate neutrophil attraction to bacterial infection and tissue injury. *Cell. Microbiol.* 14:517–528. <http://dx.doi.org/10.1111/j.1462-5822.2011.01738.x>.
 45. Colucci-Guyon E, Tinevez J-Y, Renshaw SA, Herbomel P. 2011. Strategies of professional phagocytes in vivo: unlike macrophages, neutrophils engulf only surface-associated microbes. *J. Cell Sci.* 124:3053–3059. <http://dx.doi.org/10.1242/jcs.082792>.
 46. Prajsnar TK, Cunliffe VT, Foster SJ, Renshaw S a. 2008. A novel vertebrate model of *Staphylococcus aureus* infection reveals phagocyte-dependent resistance of zebrafish to non-host specialized pathogens. *Cell. Microbiol.* 10:2312–2325. <http://dx.doi.org/10.1111/j.1462-5822.2008.01213.x>.
 47. Berthier E, Lim FY, Deng Q, Guo C-J, Kontoyiannis DP, Wang CCC, Rindy J, Beebe DJ, Huttenlocher A, Keller NP. 2013. Low-volume toolbox for the discovery of immunosuppressive fungal secondary metabolites. *PLoS Pathog.* 9:e1003289. <http://dx.doi.org/10.1371/journal.ppat.1003289>.
 48. Deng Q, Sarris M, Bennin DA, Green JM, Herbomel P, Huttenlocher A. 2013. Localized bacterial infection induces systemic activation of neutrophils through Cxcr2 signaling in zebrafish. *J. Leukoc. Biol.* 93:761–769. <http://dx.doi.org/10.1189/jlb.1012534>.
 49. Bruns S, Kniemeyer O, Hasenberg M, Aimaniananda V, Nietzsche S, Thywissen A, Jeron A, Latgé J-P, Brakhage AA, Gunzer M. 2010. Production of extracellular traps against *Aspergillus fumigatus* in vitro and in infected lung tissue is dependent on invading neutrophils and influenced by hydrophobin RodA. *PLoS Pathog.* 6:e1000873. <http://dx.doi.org/10.1371/journal.ppat.1000873>.
 50. Hohl TM, Van Epps HL, Rivera A, Morgan LA, Chen PL, Feldmesser M, Pamer EG. 2005. *Aspergillus fumigatus* triggers inflammatory responses by stage-specific beta-glucan display. *PLoS Pathog.* 1:e30. <http://dx.doi.org/10.1371/journal.ppat.0010030>.
 51. Levitz SM, Farrell TP. 1990. Human neutrophil degranulation stimulated by *Aspergillus fumigatus*. *J. Leukoc. Biol.* 47:170–175.
 52. Levitz SM, Selsted ME, Ganz T, Lehrer RI, Diamond RD. 1986. In vitro killing of spores and hyphae of *Aspergillus fumigatus* and *Rhizopus oryzae* by rabbit neutrophil cationic peptides and bronchoalveolar macrophages. *J. Infect. Dis.* 154:483–489. <http://dx.doi.org/10.1093/infdis/154.3.483>.
 53. Ambruso DR, Knall C, Abell A, Panepinto NJ, Kurkchubasche A, Thurman G, Gonzalez-Aller C, Hiester A, deBoer M, Harbeck RJ, Oyer R, Johnson GL, Roos D. 2000. Human neutrophil immunodeficiency syndrome is associated with an inhibitory Rac2 mutation. *Proc. Natl. Acad. Sci. U. S. A.* 97:4654–4659. <http://dx.doi.org/10.1073/pnas.080074897>.
 54. Bok JW, Balajee SA, Marr KA, Nielsen KF, Frisvad JC, Nancy P, Andes D, Keller NP. 2005. LaeA, a regulator of morphogenetic fungal virulence factors. *Eukaryot. Cell* 4:1574–1582. <http://dx.doi.org/10.1128/EC.4.9.1574-1582.2005>.
 55. López-Berges MS, Hera C, Sulyok M, Schäfer K, Capilla J, Guarro J, Di Pietro A. 2013. The velvet complex governs mycotoxin production and virulence of *Fusarium oxysporum* on plant and mammalian hosts. *Mol. Microbiol.* 87:49–65. <http://dx.doi.org/10.1111/mmi.12082>.
 56. Wu D, Oide S, Zhang N, Choi MY, Turgeon BG. 2012. ChLae1 and ChVel1 regulate T-toxin production, virulence, oxidative stress response, and development of the maize pathogen *Cochliobolus heterostrophus*. *PLoS Pathog.* 8:e1002542. <http://dx.doi.org/10.1371/journal.ppat.1002542>.
 57. Wiemann P, Brown DW, Kleigrew K, Bok JW, Keller NP, Humpf H-U, Tudzynski B. 2011. FVel1 and FLae1, components of a velvet-like complex in *Fusarium fujikuroi*, affect differentiation, secondary metabolism and virulence. *Mol. Microbiol.* 77:972–994. <http://dx.doi.org/10.1111/j.1365-2958.2010.07263.x>.
 58. Sugui Y, Pardo J, Chang YC, Müllbacher A, Zarembek K a, Galvez EM, Brinster L, Zervas P, Gallin JI, Simon MM, Kwon-Chung KJ. 2007. Role of laeA in the regulation of alb1, gliP, conidial morphology, and virulence in *Aspergillus fumigatus*. *Eukaryot. Cell* 6:1552–1561. <http://dx.doi.org/10.1128/EC.00140-07>.
 59. Dagenais TRT, Giles SS, Aimaniananda V, Latgé J-P, Hull CM, Keller NP. 2010. *Aspergillus fumigatus* LaeA-mediated phagocytosis is associated with a decreased hydrophobin layer. *Infect. Immun.* 78:823–829. <http://dx.doi.org/10.1128/IAI.00980-09>.
 60. Ben-Ami R, Lewis RE, Leventakos K, Kontoyiannis DP. 2009. *Aspergillus fumigatus* inhibits angiogenesis through the production of gliotoxin and other secondary metabolites. *Blood* 114:5393–5399. <http://dx.doi.org/10.1182/blood-2009-07-231209>.
 61. Jahn B, Koch A, Schmidt A, Wanner G, Gehringer H, Bhakdi S, Brakhage AA. 1997. Isolation and characterization of a pigmentless-conidium mutant of *Aspergillus fumigatus* with altered conidial surface and reduced virulence. *Infect. Immun.* 65:5110–5117.
 62. Jahn B, Langfelder K, Schneider U, Schindel C, Brakhage AA. 2002. PKSP-dependent reduction of phagolysosome fusion and intracellular kill of *Aspergillus fumigatus* conidia by human monocyte-derived macrophages. *Cell. Microbiol.* 4:793–803. <http://dx.doi.org/10.1046/j.1462-5822.2002.00228.x>.
 63. Thywissen A, Heinekamp T, Dahse H-M, Schmalder-Ripcke J, Nietzsche S, Zipfel PF, Brakhage AA. 2011. Conidial dihydroxynaphthalene melanin of the human pathogenic fungus *Aspergillus fumigatus* interferes with the host endocytosis pathway. *Front. Microbiol.* 2:96. <http://dx.doi.org/10.3389/fmicb.2011.00096>.
 64. Chai LY a, Netea MG, Sugui J, Vonk AG, van de Sande WWJ, Warris A, Kwon-Chung KJ, Kullberg BJ. 2010. *Aspergillus fumigatus* conidial melanin modulates host cytokine response. *Immunobiology.* 215:915–920. <http://dx.doi.org/10.1016/j.imbio.2009.10.002>.

65. Aimaniananda V, Bayry J, Bozza S, Kniemeyer O, Perruccio K, Elluru SR, Clavaud C, Paris S, Brakhage AA, Kaveri SV, Romani L, Latgé J-P. 2009. Surface hydrophobin prevents immune recognition of airborne fungal spores. *Nature* 460:1117–1121. <http://dx.doi.org/10.1038/nature08264>.
66. Danilova N, Steiner LA. 2002. B cells develop in the zebrafish pancreas. *Proc. Natl. Acad. Sci. U. S. A.* 99:13711–13716. <http://dx.doi.org/10.1073/pnas.212515999>.
67. Willett CE, Cortes A, Zuasti A, Zapata AG. 1999. Early hematopoiesis and developing lymphoid organs in the zebrafish. *Dev. Dyn.* 214:323–336. [http://dx.doi.org/10.1002/\(SICI\)1097-0177\(199904\)214:4<323::AID-AJA5>3.0.CO;2-3](http://dx.doi.org/10.1002/(SICI)1097-0177(199904)214:4<323::AID-AJA5>3.0.CO;2-3).
68. Clay H, Davis JM, Beery D, Huttenlocher A, Lyons SE, Ramakrishnan L. 2007. Dichotomous role of the macrophage in early *Mycobacterium marinum* infection of the zebrafish. *Cell Host Microbe* 2:29–39. <http://dx.doi.org/10.1016/j.chom.2007.06.004>.
69. Rounioja S, Saralahti A, Rantala L, Parikka M, Henriques-Normark B, Silvennoinen O, Rämetsä M. 2012. Defense of zebrafish embryos against *Streptococcus pneumoniae* infection is dependent on the phagocytic activity of leukocytes. *Dev. Comp. Immunol.* 36:342–348. <http://dx.doi.org/10.1016/j.dci.2011.05.008>.
70. Amich J, Schaffner L, Haas H, Krappmann S. 2013. Regulation of sulphur assimilation is essential for virulence and affects iron homeostasis of the human-pathogenic mould *Aspergillus fumigatus*. *PLoS Pathog.* 9:e1003573. <http://dx.doi.org/10.1371/journal.ppat.1003573>.
71. Zarembek KA, Sugui JA, Chang YC, Kwon-Chung KJ, Gallin JI. 2007. Human polymorphonuclear leukocytes inhibit *Aspergillus fumigatus* conidial growth by lactoferrin-mediated iron depletion. *J. Immunol.* 178:6367–6373. <http://dx.doi.org/10.4049/jimmunol.178.10.6367>.
72. Bullen JJ. 1981. The significance of iron in infection. *Rev. Infect. Dis.* 3:1127–1138. <http://dx.doi.org/10.1093/clinids/3.6.1127>.
73. McCormick A, Loeffler J, Ebel F. 2010. *Aspergillus fumigatus*: contours of an opportunistic human pathogen. *Cell. Microbiol.* 12:1535–1543. <http://dx.doi.org/10.1111/j.1462-5822.2010.01517.x>.
74. Balloy V, Chignard M. 2009. The innate immune response to *Aspergillus fumigatus*. *Microbes Infect.* 11:919–927. <http://dx.doi.org/10.1016/j.micinf.2009.07.002>.
75. Carradice D, Lieschke GJ. 2008. Zebrafish in hematology: sushi or science? *Blood* 111:3331–3342. <http://dx.doi.org/10.1182/blood-2007-10-052761>.
76. Luther K, Torosantucci A, Brakhage AA, Heesemann J, Ebel F. 2007. Phagocytosis of *Aspergillus fumigatus* conidia by murine macrophages involves recognition by the dectin-1 beta-glucan receptor and Toll-like receptor 2. *Cell. Microbiol.* 9:368–381. <http://dx.doi.org/10.1111/j.1462-5822.2006.00796.x>.
77. Lorenz MC, Bender JA, Fink GR. 2004. Transcriptional response of *Candida albicans* upon internalization by macrophages. *Eukaryot. Cell* 3:1076–1087. <http://dx.doi.org/10.1128/EC.3.5.1076-1087.2004>.
78. Lim FY, Hou Y, Chen Y, Oh J-H, Lee I, Bugni TS, Keller NP. 2012. Genome-based cluster deletion reveals an endocrocin biosynthetic pathway in *Aspergillus fumigatus*. *Appl. Environ. Microbiol.* 78:4117–4125. <http://dx.doi.org/10.1128/AEM.07710-11>.
79. Nierman WC, Pain A, Anderson MJ, Wortman JR, Kim HS, Arroyo J, Berriman M, Abe K, Archer DB, Bermejo C, Bennett J, Bowyer P, Chen D, Collins M, Coulson R, Davies R, Dyer PS, Farman M, Fedorova N, Fedorova N, Feldblyum TV, Fischer R, Fosker N, Fraser A, García JL, García MJ, Goble A, Goldman GH, Gomi K, Griffith-Jones S, Gwilliam R, Haas B, Haas H, Harris D, Horiuchi H, Huang J, Humphray S, Jiménez J, Keller N, Khouri H, Kitamoto K, Kobayashi T, Konzack S, Kulkarni R, Kumagai T, Lafon A, Lafton A, Latgé J-P, Li W, Lord A, Lu C, Majoros WH, May GS, Miller BL, Mohamoud Y, Molina M, Monod M, Mouyna I, Mulligan S, Murphy L, O'Neil S, Paulsen I, Peñalva MA, Perteau M, Price C, Pritchard BL, Quail MA, Rabbinowitsch E, Rawlins N, Rajandream M-A, Reichard U, Renaud H, Robson GD, Rodríguez de Córdoba S, Rodríguez-Peña JM, Ronning CM, Rutter S, Salzberg SL, Sanchez M, Sánchez-Ferrero JC, Saunders D, Seeger K, Squares R, Squares S, Takeuchi M, Tekaiia F, Turner G, Vazquez de Aldana CR, Weidman J, White O, Woodward J, Yu J-H, Fraser C, Galagan JE, Asai K, Machida M, Hall N, Barrell B, Denning DW. 2005. Genomic sequence of the pathogenic and allergenic filamentous fungus *Aspergillus fumigatus*. *Nature* 438:1151–1156. <http://dx.doi.org/10.1038/nature04332>.
80. Hartmann T, Sasse C, Schedler A, Hasenberg M, Gunzer M, Krappmann S. 2011. Shaping the fungal adaptome—stress responses of *Aspergillus fumigatus*. *Int. J. Med. Microbiol.* 301:408–416. <http://dx.doi.org/10.1016/j.ijmm.2011.04.008>.
81. Steele C, Rapaka RR, Metz A, Pop SM, Williams DL, Gordon S, Kolls JK, Brown GD. 2005. The beta-glucan receptor dectin-1 recognizes specific morphologies of *Aspergillus fumigatus*. *PLoS Pathog.* 1:e42. <http://dx.doi.org/10.1371/journal.ppat.0010042>.
82. Eisen JS, Smith JC. 2008. Controlling morpholino experiments: don't stop making antisense. *Development* 135:1735–1743. <http://dx.doi.org/10.1242/dev.001115>.
83. Bok JW, Noordermeer D, Kale SP, Keller NP. 2006. Secondary metabolic gene cluster silencing in *Aspergillus nidulans*. *Mol. Microbiol.* 61:1636–1645. <http://dx.doi.org/10.1111/j.1365-2958.2006.05330.x>.
84. Jain S, Keller N. 2013. Insights to fungal biology through *LaeA* sleuthing. *Fungal Biol. Rev.* 27:51–59. <http://dx.doi.org/10.1016/j.fbr.2013.05.004>.
85. Yin W-B, Baccile JA, Bok JW, Chen Y, Keller NP, Schroeder FC. 2013. A nonribosomal peptide synthetase-derived iron(III) complex from the pathogenic fungus *Aspergillus fumigatus*. *J. Am. Chem. Soc.* 135:2064–2067. <http://dx.doi.org/10.1021/ja311145n>.